The Iranian Journal of Mechanical Engineering Transactions of ISME
Journal homepage: https://jmee.isme.ir/
Vol. 26, No. 2, 2025, pp. 72-92

Research Paper

DOI: https://doi.org/10.30506/jmee.2025.2040212.1361

A Modeling Framework for Rigid Legs Passive Dynamic Biped Walkers in MSC ADAMS

Roozbeh Ghanadi Azar*
M.Sc.

Kourosh Moeini†
B.Sc.

Mohammad Reza Haghjoo‡
Assistant Professor

Mostafa Taghi Zadeh§
Associate Professor

Passive dynamic walkers have gained widespread interest for their ability to mimic human-like movements. However, modeling and simulating these walkers in mathematical software can be challenging due to their complex dynamic equations of motions. This paper presents a framework for multibody modeling and simulating passive dynamic biped walkers with rigid legs in MSC ADAMS. This approach significantly simplifies the modeling process by avoiding the complexity of deriving mathematical equations of motion. The framework involves creating a general base model of the biped walker (such as a compass-like design), followed by dynamic analysis in MSC ADAMS. The model developed in MSC ADAMS is carefully adapted through a suggested parameter adjustment procedure to ensure that the core functionalities of a purely mathematical model are preserved. The findings indicate that a slightly higher initial angular velocity of the stance leg is required in MSC ADAMS compared to the mathematical model to achieve stable periodic motion and account for stance foot slippage. This research enables more realistic simulations of passive biped robots in MSC ADAMS, reducing reliance on purely theoretical models.

Keywords: Passive dynamic walker, Compass biped walker, MSC ADAMS, Modeling, Periodic motions

1 Introduction

Limit cycle walking biped robots are emerging as formidable contenders to ZMP-based humanoid robots due to their practical and natural walking [1-5].

*M.Sc., Faculty of Mechanical and Energy Engineering, Shahid Beheshti University, Tehran, Iran, roozbehazar75@hotmail.com
†B.Sc., Faculty of Mechanical and Energy Engineering, Shahid Beheshti University, Tehran, Iran, kourosh.moeini.sut@gmail.com
‡Corresponding author, Assistant Professor, Faculty of Mechanical and Energy Engineering, Shahid Beheshti University, Tehran, Iran, m_haghjoo@sbu.ac.ir
§Associate Professor, Faculty of Mechanical and Energy Engineering, Shahid Beheshti University, Tehran, Iran, mo_taghizadeh@sbu.ac.ir

Received: 2024/09/02, Revised: 2024/12/29, Accepted: 2025/01/13

These robots can exhibit stable limit cycle gaits without continuous local controllability during motion [6]. The concept of limit cycle walking originated from McGeer's influential research, which revealed walking as a naturally occurring dynamic mode triggered solely by gravity in a collection of mechanical systems, classified as "passive dynamic walkers" [7]. Ongoing research in passive dynamic walkers has theoretically and practically expanded since McGeer's work [8]. Garcia et al. [9] introduced the simplest walking model, capable of passive descent on a shallow slope. Goswami et al. [10] considered a compass-like model with the upper body, demonstrating stable passive walking. One of the main challenges in passive dynamic walkers is the theoretical extraction of their dynamic equations or models. Many researchers have struggled with the complexity and formidable task of obtaining fully analytical equations for these robots [11]. Recently, multibody dynamic simulation software has been developed to physically model systems instead of extracting complex equations of motion. Undoubtedly, one of the most powerful and well-known of these software is MSC ADAMS [12, 13]. It allows the user to simulate the motion of any complex mechanical system. It presents detailed velocity and displacement information for each moving body, joint dynamic forces, and so on [14]. Hence, a useful examination and optimization of any dynamic system -before accurate costly prototyping and experiment- can be accomplished using MSC ADAMS [15, 16]. Using multibody simulation software like ADAMS can significantly facilitate and accelerate the modeling stage of passive walkers. Researchers can avoid the complexity of deriving mathematical equations of motion for the walker and instead focus on physically assembling its CAD part models.

Many researchers have explored the modeling of industrial robots, such as PUMA and KUKA [17, 18], in MSC ADAMS. Additionally, studies [19-28] highlight the extensive use of MSC ADAMS for simulating active exoskeletons and rehabilitation-oriented systems, focusing on controllers, actuators, and human-exoskeleton interactions. However, the application of MSC ADAMS for modeling biped robots remains limited and fraught with significant challenges. Zhu et al. [29] investigated a simplified humanoid robot with elastic feet in MSC ADAMS, integrated with a PID controller in MATLAB for co-simulation. They found substantial discrepancies between the simulation results from MATLAB and MSC ADAMS. Similarly, Hashemi et al. [30] compared the analytical inverse dynamics of the Nao humanoid robot's lower body, modeled in MATLAB, with MSC ADAMS simulation results for two scenarios. Both studies centered on ZMP-based biped robots. The challenges are even more pronounced when modeling passive dynamic biped walkers in MSC ADAMS, which rely solely on gravitational forces for locomotion [31]. Modeling the dynamic behavior of rigid-legged passive walkers poses significant difficulties, particularly in accounting for impacts and foot slippage during stance phases. Analytical models, such as those implemented in MATLAB, often rely on idealized assumptions that are not easily adaptable to these challenges [32]. In MSC ADAMS, the impact model is based on Hertzian contact theory, representing collisions as spring-damper systems that approximate non-plastic collisions [33]. In contrast, MATLAB models typically assume fully plastic ideal collisions [34]. This fundamental difference in impact modeling results in unavoidable discrepancies between the simulation outputs of these two software environments. Ylikorpi et al. [35] compared a rigid-legged passive kneed walker modeled in MATLAB with ADAMS MD R3. They reported significant deviations, especially during the knee-lock phase, where ADAMS simulations were also highly noisy. Their findings suggest that reproducing MATLAB results in ADAMS for rigid-legged passive walkers is only partially feasible. Vasileiou et al. [36] developed a digital twin of a passive biped robot using analysis, experiments, and MSC ADAMS simulations. However, their model employed non-rigid, flexible legs with curved feet, reducing overall stiffness to minimize computational effort and discrepancies. This approach omitted the instantaneous impact phase essential for mathematical modeling of rigid-legged passive biped walkers.

Hence, a satisfactory agreement between multibody dynamics simulations and mathematical models of passive biped robots with rigid legs remains elusive, underscoring a significant research gap in effectively leveraging multibody modeling tools like ADAMS. This research addresses this gap by utilizing dynamic multibody simulation environments such as MSC ADAMS to model rigid-legged passive dynamic walkers, incorporating fully plastic instantaneous impact phases. Essential guidelines and parameter adjustments are introduced to align the multibody model in MSC ADAMS more closely with the MATLAB mathematical model. The robustness and reliability of the proposed ADAMS model are validated through results comparable to MATLAB simulations. A two-link model is used as a foundational example to demonstrate the feasibility of these parameter adjustments and the general modeling process. The principles established here can be extended to more complex passive biped models, offering a generalized framework for validation and fine-tuning. This research lays the groundwork for a more realistic yet straightforward approach to modeling and verifying passive biped walkers in MSC ADAMS, reducing dependence on theoretical models and the extraction of complex equations of motion. The rest of the paper is reported as follows: Section (2) presents the passive walker model. Then, the mathematical model and periodic motions are presented using MATLAB in Section (3). Section (4) describes how to model and simulate a rigid-legged passive dynamic walker in MSC ADAMS. Section (5) compares and discusses the results obtained from MATLAB and MSC ADAMS. Finally, a conclusion is presented.

2 Passive walker model

The model used in this study is a two-rigid link compass biped walker (CBW), as shown in Figure (1). The robot model has two dimensions, with motion occurring on a slope.

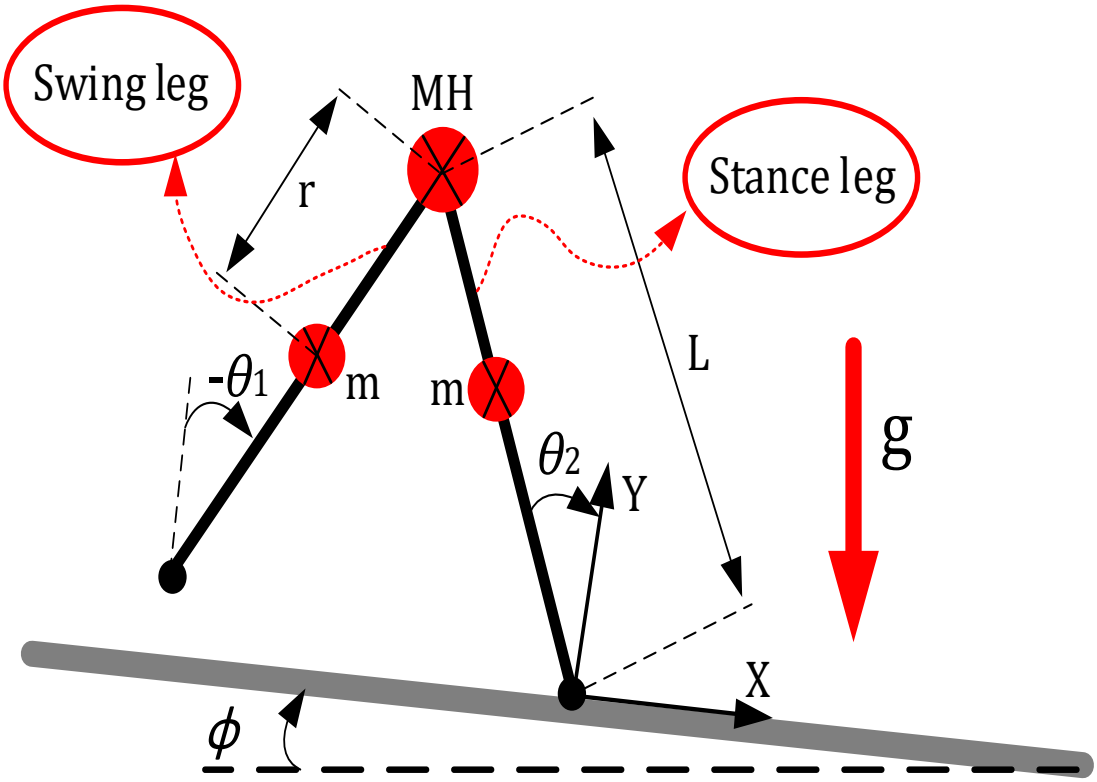

Figure 1 Compass point-feet biped walker as the basic model for the study

Table 1 The physical parameters of the CBW

Parameters	Units	Value
Length of legs (L)	m	1
Mass of legs (m)	kg	5
Mass of hip (MH)	kg	10
Gravity (g)	m/s^2	9.81

In the figure, the stance and swing leg angles are denoted as θ_2 and θ_1, respectively. Geometric parameters, physical specifications of the robot, and the slope's degree (φ) are illustrated in Figure (1), with numerical values provided in Table (1) [10]. Notably, the mass of the links is concentrated and placed in the middle of the legs. Assumptions for this robot model include: 1-All links of the robot are rigid, 2-The only joint of this robot (hip joint) is frictionless.

3 Dynamic modeling in MATLAB

Each stride of the robot's walking consists of two steps. Each step also includes two motion phases: 1) the continuous phase and 2) the impact phase. In the continuous phase, one leg is in contact with the ground (stance leg), and the other moves forward in a hanging position. After the swing leg reaches the ground, a collision occurs, called the impact phase. The next step begins similarly but with a role reversal of the stance and swing leg.

3.1 Continuous phase

The assumptions considered in this phase include: 1-The friction between the ground and the leg in contact with it is significant enough that the leg does not slip, 2-The reaction force between the stance leg and the ground always remains positive (upward). The state variables are expressed as Equation (1), given the provided explanations.

$$\boldsymbol{x} = \begin{bmatrix} \boldsymbol{q} \\ \dot{\boldsymbol{q}} \end{bmatrix} = \begin{bmatrix} \theta_1 \\ \theta_2 \\ \dot{\theta}_1 \\ \dot{\theta}_2 \end{bmatrix} \tag{1}$$

Where $\boldsymbol{q}$ in the aboveequation represents the robot's positional variables (generalized coordinates). The Lagrange method is used to derive the governing dynamic equations for this robot as [37]

$$\frac{d}{dt}\left(\frac{\partial L}{\partial \dot{\boldsymbol{q}}_i}\right) - \frac{\partial L}{\partial \boldsymbol{q}_i} = \boldsymbol{F}_i \tag{2}$$

L is the LaGrange, and $\boldsymbol{F}_i$ is the equation's generalized force vector associated with $\boldsymbol{q}$. Appendix A gives details of the position and velocity vectors and the model's kinetic and potential energies. Finally, the governing equations will be obtained as equation (3) [37].

$$\boldsymbol{D}(\boldsymbol{q})\ddot{\boldsymbol{q}} + \boldsymbol{C}(\boldsymbol{q}, \dot{\boldsymbol{q}})\dot{\boldsymbol{q}} + \boldsymbol{G}(\boldsymbol{q}) = \boldsymbol{B}(\boldsymbol{q})\boldsymbol{u} \tag{3}$$

Where $\boldsymbol{D}$ is the inertia matrix, $\boldsymbol{C}$ is the Coriolis matrix, $\boldsymbol{G}$ is the gravity vector, $\boldsymbol{u}$ is the actuator torque vector, and $\boldsymbol{B}$ is the matrix that converts actuator torques to generalized forces. Here,

due to passive walking and the lack of an actuator in the robot, $\boldsymbol{u} = 0$. Furthermore, the matrices of $\boldsymbol{D}$, $\boldsymbol{C}$, and $\boldsymbol{G}$ are detailed in Appendix A. Then, the dynamic state-space model of the robot is obtained as:

$$\dot{\boldsymbol{x}} = \begin{bmatrix} \dot{\boldsymbol{q}} \\ \ddot{\boldsymbol{q}} \end{bmatrix} = \begin{bmatrix} \dot{\boldsymbol{q}} \\ \boldsymbol{D}(\boldsymbol{q})^{-1}[-\boldsymbol{C}(\boldsymbol{q}, \dot{\boldsymbol{q}})\dot{\boldsymbol{q}} - \boldsymbol{G}(\boldsymbol{q})] \end{bmatrix} \tag{4}$$

3.2 Impact phase

In this phase, simplified assumptions have also been used for the dynamic model. These assumptions include [34]:

- During the impact of the swing leg on the ground, the leg neither slips nor jumps upwards but immediately reaches zero velocity at the contact point.
- The impact is assumed to be immediate.
- Impulsive forces immediately change the speeds of the links but do not create any change in the positions of the links.

We first need to obtain the system's dynamic equations in general form to model the impact without considering additional constraints such as pinning the stance leg to the ground. In this case, the system has 4 degrees of freedom, with 2 degrees of freedom related to the positional location of the stance leg's toe and 2 degrees of freedom related to the angles between the links. These are represented in C (5).

$$\boldsymbol{q_e} = \begin{bmatrix} x \\ y \\ \boldsymbol{q} \end{bmatrix} \tag{5}$$

Consequently, the governing equations in the impact phase will be obtained as

$$\boldsymbol{D_e}(\boldsymbol{q_e})\ddot{\boldsymbol{q}}_{\boldsymbol{e}} + \boldsymbol{C_e}(\boldsymbol{q_e}, \dot{\boldsymbol{q}}_{\boldsymbol{e}})\dot{\boldsymbol{q}}_{\boldsymbol{e}} + \boldsymbol{G_e}(\boldsymbol{q_e}) = \boldsymbol{\delta F_{ext}} \tag{6}$$

$\boldsymbol{D_e}, \boldsymbol{C_e}, and\ \boldsymbol{G_e}$ matrices are computable as in the impact phase and bring the matrices of them in Appendix A. In the above equation, $\boldsymbol{\delta F_{ext}}$ represents the impulsive generalized forces that arise due to the impact of the suspended foot on the ground. The resulting equation is obtained as Appendix A if we integrate the above equation throughout the impact. If we denote the position of the swing leg's foot tip as $\boldsymbol{P}(\boldsymbol{q_e})$, then taking a partial derivative led to Appendix A. Given the assumptions of the impact model, the swing leg does not slip or jump upwards after the impact on the ground. Therefore, this assumption is modeled as Equation (7).

$$\boldsymbol{E}\dot{\boldsymbol{q}}_{\boldsymbol{e}}^{+} = 0 \tag{7}$$

Thus, to obtain the velocities after the impact on the ground, the system of linear equations must be solved as in Appendix A. By solving this equation, the velocities can be immediately obtained after the impact.

$$\boldsymbol{x}^{+} = \Delta(\boldsymbol{x}^{-}) \tag{8}$$

It is crucial to note that the roles of the stance and swing legs switch after the impact. Now, considering the points mentioned above, the overall dynamic equation of the system can be written as a combination of the continuous and impact phases.

$$\begin{cases} \dot{\boldsymbol{x}}(\boldsymbol{t}) = \boldsymbol{f}(\boldsymbol{x}(\boldsymbol{t})) & \boldsymbol{x}^{-}(\boldsymbol{t}) \notin S \\ \boldsymbol{x}^{+}(\boldsymbol{t}) = \Delta(\boldsymbol{x}^{-}(\boldsymbol{t})) & \boldsymbol{x}^{-}(\boldsymbol{t}) \in S \end{cases} \tag{9-1}$$

$$S = \{(\boldsymbol{q}, \dot{\boldsymbol{q}}) | \theta_1 = -\theta_2\} \tag{9-2}$$

Where $\boldsymbol{f}(\boldsymbol{x})$ are extracted in the Appendix in detail, the subspace S is a hypersurface in the state space where the impact phase occurs. This corresponds to the condition $\theta_1 = -\theta_2$ for the leg's impact on the ground. This means the impact occurs when the swing leg's angle reaches the stance leg's complementary angle. It should be noted that to achieve such a condition, we do not consider the scuffing with the ground.

3.3 Periodic motion and fixed points

One standard method for analyzing the existence and stability of periodic motions in walking robots is the Poincaré map [38]. It relates the system's state immediately after a collision (the beginning of a step) to the state after the subsequent collision (the beginning of the next step) [14, 39].

$$\boldsymbol{x_{n+1}} = \boldsymbol{P}(\boldsymbol{x_n}) \tag{10}$$

A fixed point represents a state of the system corresponding to a periodic motion or limit cycle. If this fixed point is stable, the gait is also stable. To establish stability, the eigenvalues of the P map at the fixed point must be less than one [40]. Numerical methods are commonly used to prove this condition. To simulate the CBW in MATLAB, the dynamic equations and the Poincaré map are coded [41]. Determining the fixed point of the Poincaré map is crucial for the robot to walk stably and periodically on an inclined plane. We employ MATLAB's "fsolve" function for numerical optimization [42, 43]. Initially, random values are considered for the state variables, and the optimization reveals the desired values that result in a stable periodic motion or fixed point for the robot.
Under the above conditions, the asymptotically stable walking of the theoretical model of the bipedal robot under study was simulated in MATLAB software.

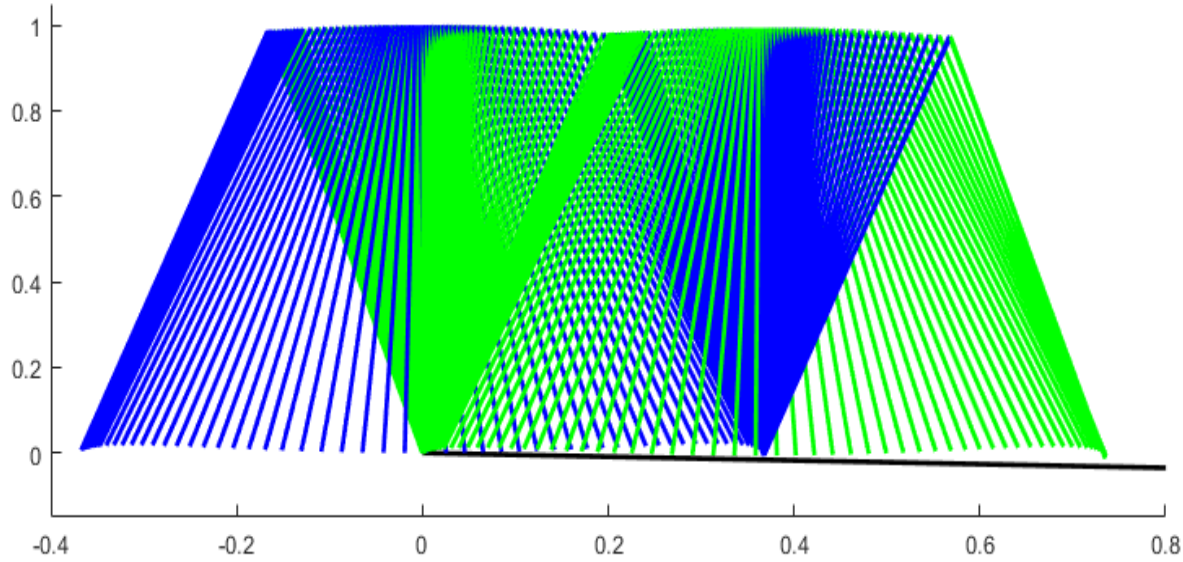

Figure 2 Stick diagram for one gait cycle of CBW in MATLAB

Figure (2) illustrates snapshots of the model during one gait cycle of motion in MATLAB.

$$\boldsymbol{x_p} = \begin{bmatrix} \theta_1 \\ \theta_2 \\ \dot{\theta_1} \\ \dot{\theta_2} \end{bmatrix} = \begin{bmatrix} -0.2022 \\ 0.1674 \\ -0.60 \\ -0.84 \end{bmatrix} \tag{11}$$

Under the above conditions, the asymptotically stable walking of the theoretical model of the bipedal robot under study was simulated in MATLAB software. Figure (2) illustrates snapshots of the model during one gait cycle of motion in MATLAB.

4 Dynamic modeling in MSC ADAMS

This section uses the passive walker model in MSC ADAMS to match the previous mathematical model and validate the obtained results. MSC ADAMS utilizes the recursive formulation of Newton-Euler mechanics combined with multibody dynamics principles for modeling. Unlike MATLAB's Lagrangian approach, its recursive handling of dynamics and constraint equations ensures scalability without requiring a complete remodel when adding links. This highlights the practicality and user-friendliness of MSC ADAMS. Furthermore, MSC ADAMS simulates collisions and ground contacts using spring-damper and Hertzian contact theories, providing a realistic representation of real-world conditions.

The overall model created in MSC ADAMS, including the biped and the terrain, is shown in Figure (3). The robot consists of three straight, rigid links: the right, left leg, and hip. The hip consists of a rod that acts as a revolute joint. All the model links under study were CAD modeled in SolidWorks based on the geometric parameters explained in Section (2). Once the model is created, the movement of the robot is constrained by defining a plane constraint; thus, the robot's gait is executed in a 2-dimensional space. One of the challenges in MSC ADAMS is the 3D environment, while we need to simulate a 2D walking model similar to the theoretical model in MATLAB [31]. To overcome this problem, we model a leg as two symmetric rigid links fixed and constrained to each other, as shown in Figure (3), which restricts the motion of the whole robot to the 2D plane. After importing the modeled links into MSC ADAMS, we placed the link acting as the swing leg (link-leg 1) between the other two links (link-leg 2) and bound them by a revolute joint in the hip (link-hip). In addition, we matched the physical and geomatic parameters of each link of CBW in MSC ADAMS to the MATLAB model exactly (Figure (4a)). As shown in Figure (4a) , and consistent with the MATLAB implementation, we employ a point mass model with inertia values intentionally set to zero in MSC ADAMS. This framework can also be adapted to accommodate more complex models beyond the point mass representation.

To position the walker correctly on the ground in MSC ADAMS, we have temporarily connected the feet-point of the stance leg and the ground by a revolute joint, as shown in Figure (3). Note that this joint was later deactivated before several steps were simulated. In addition, the terrain was modeled as a checkerboard-like surface to avoid the foot touching down on the ground, as shown in Figure (3). The robot's gait does not include toe and heel rotation, as the movement phases only include the rolling phase. A challenge in this section was to determine the location of scuffing on the ground. To solve this problem, we extracted the length of each step from MATLAB and created the physical ground based on this. Another major challenge is that the impact model of MSC ADAMS is based on Hertzian contact theory, and the impact of CBW on the ground cannot be fully inelastic like the ideal model assumed in MATLAB [33, 34]. The Hertzian relationship refers to the mathematical model proposed by Heinrich Rudolf to describe the behavior of elastic materials on contact [33].

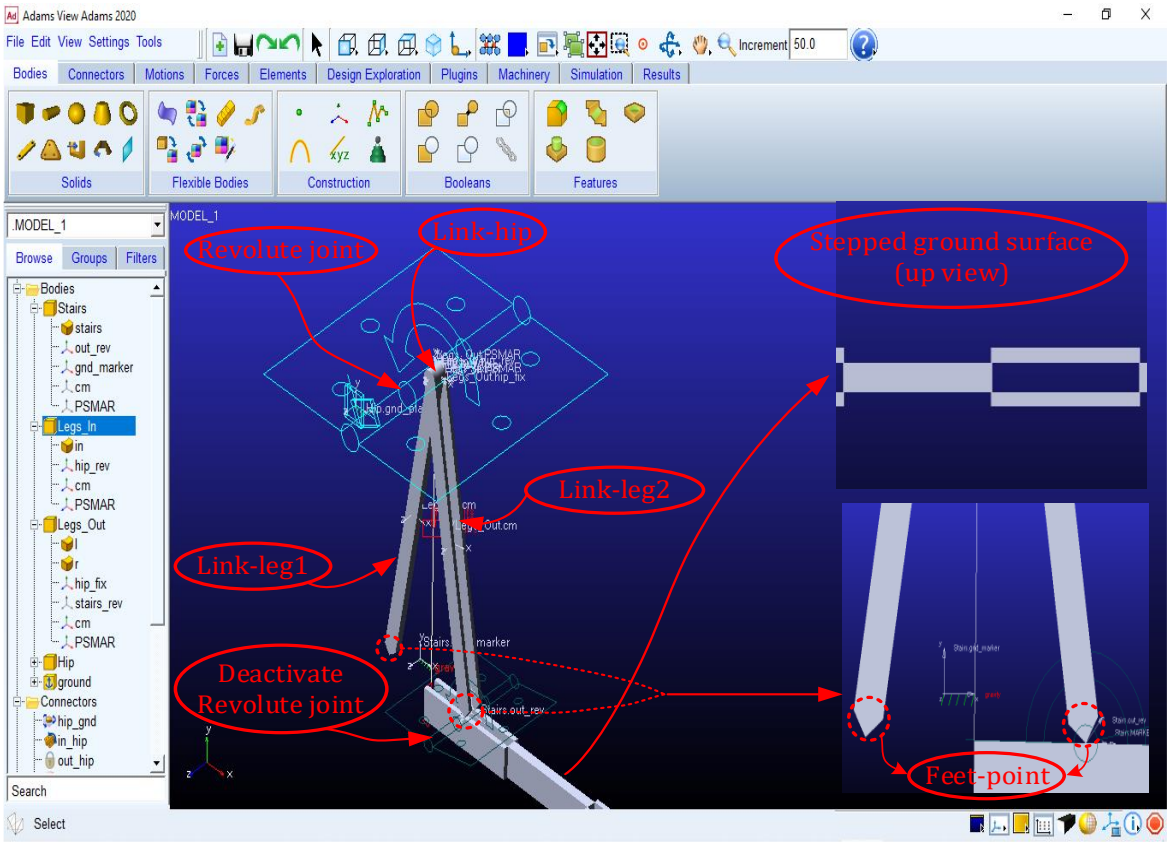

Figure 3 Dynamic model of CBW in MSC ADAMS

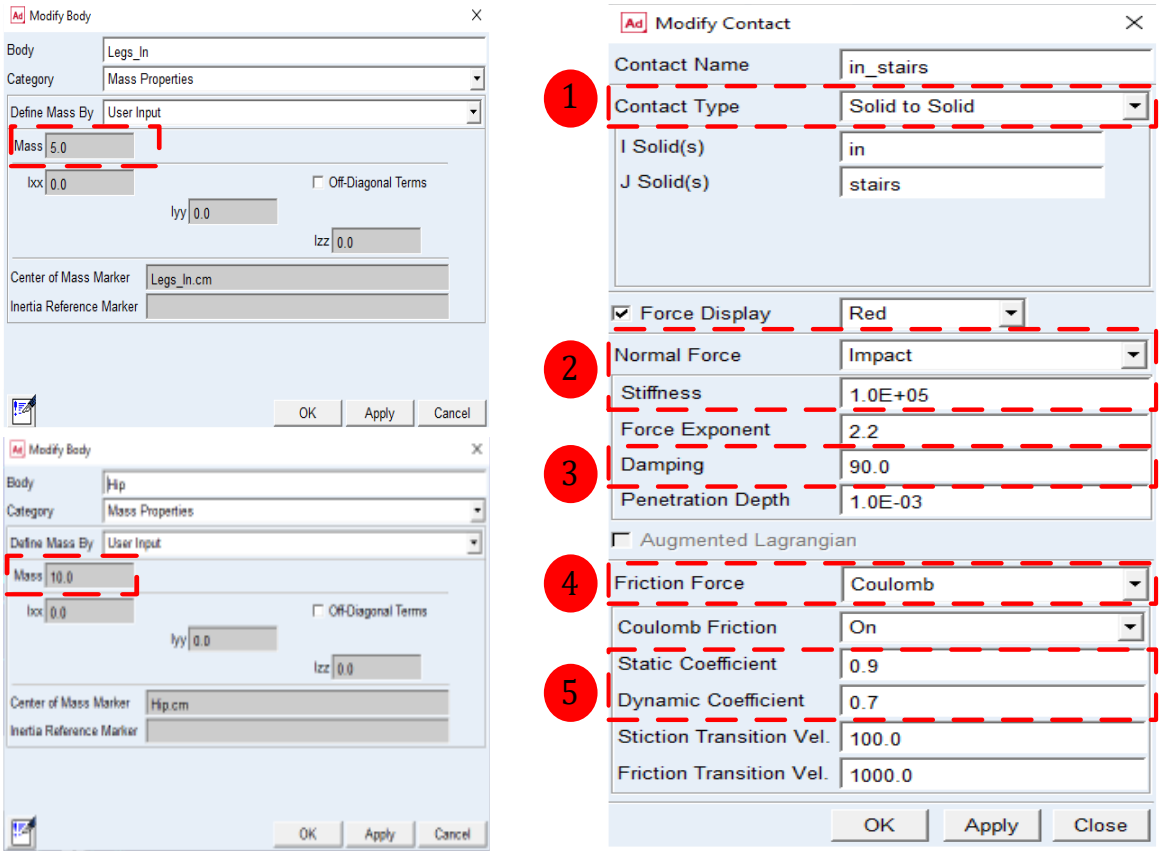

(a) **(b)**

Figure 4 Values entered for (**a**) Geometrical and physical parameters and (**b**) Impact and friction coefficients [12]

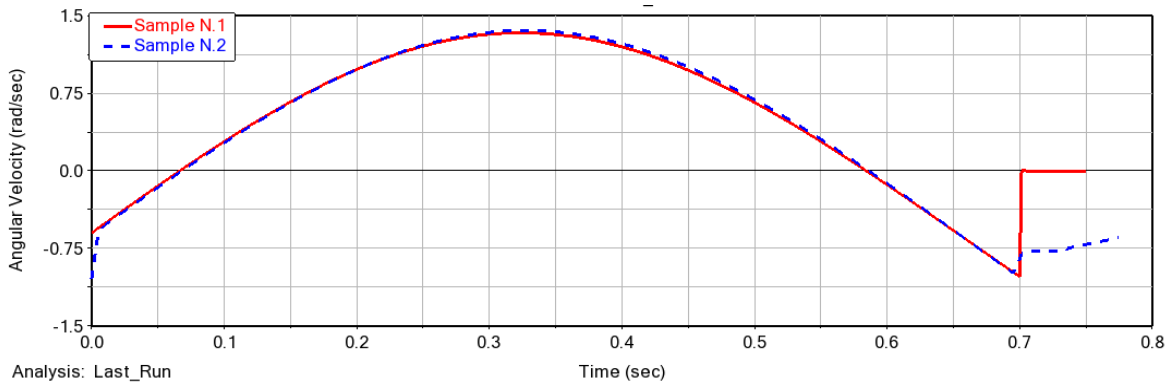

(**a**)

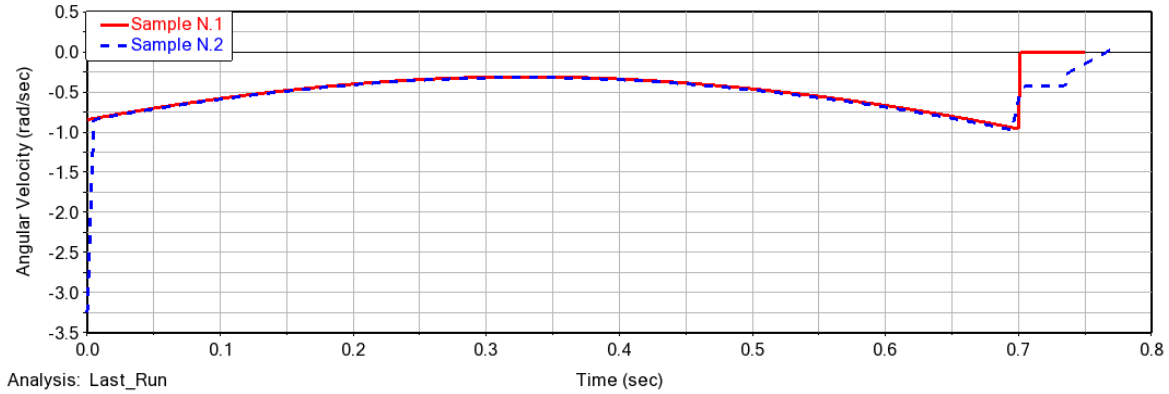

(**b**)

Figure 5 The final initial angular velocity plots of (**a**) link 1 and (**b**) link 2

Table 2 The initial values of the state space variable vectors in MATLAB and MSC ADAMS

	MATLAB	MSC ADAMS	Difference rate percent
$\boldsymbol{\theta_1\ (rad)}$	-0.2022	-0.2021	+0.1%
$\boldsymbol{\theta_2\ (rad)}$	0.1674	0.1670	+0.15%
$\boldsymbol{\dot{\theta}_1\left(rad/sec\right)}$	-0.60	-1.02	+41%
$\boldsymbol{\dot{\theta}_2\left(rad/sec\right)}$	-0.84	-3.20	+74%

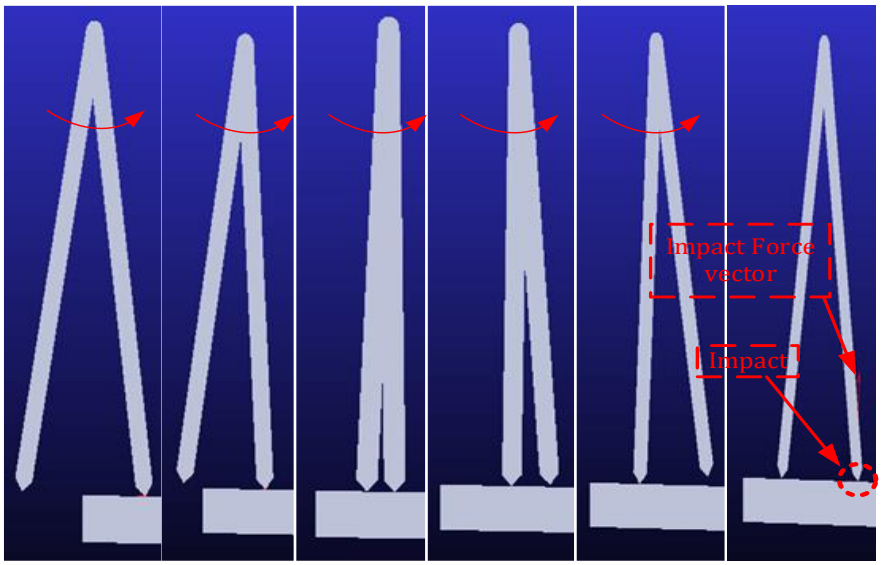

Figure 6 Snapshot of periodic walking of CBW for one gait cycle in MSC ADAMS

The relationship describes the contact area, deformation, and stress distribution between two elastic bodies in contact, assuming that the deformation is within the elastic limit of the materials [44]. We have tried to achieve an ideal situation in which the contact does not cause any significant sliding or bouncing, and the mechanism can ideally perform periodic walking [45]. In order to have enough friction in the MSC ADAMS model at the feet on the one hand and to maintain the similarity with the ideal model in MATLAB on the other hand, we consider minor foot points beveled with a radius of 1 mm in the CAD model as shown in Figure (3).
Additionally, as shown in Figure (4b), MSC ADAMS provides various contact options, such as surface-to-solid, curve-to-solid, and solid-to-solid, all based on spring-damper and Hertzian contact theory. For this study, we chose the solid-to-solid type to closely mirror real-world conditions while maintaining computational efficiency. In the collision dialog box, we also set the contact type to fixed, the normal force to impact, the friction force to coulomb, and the values of stiffness, damping, and static and dynamic friction between the feet-point and the ground to 10^5, 90, 0.9 and 0.7, respectively [46]. After all the above steps, we study CBW's behavior when walking on a slope in MSC ADAMS. In the first phase, we temporarily inserted a revolute joint between the initial stance foot and the ground. We simulated the model for one step using the same initial conditions as the theoretical model in MATLAB [47]. In this case, there would be no slippage between the stance foot and the ground, and the robot would not slide. We simulated the model several times under the assumed conditions. However, we had several failures, mainly due to the insufficient initial angular velocity of the legs, which caused the robot to lose balance after one step.
Consequently, we started to increase the initial angular velocities of the legs. As a result, we were able to achieve stable periodic motion and equalize the state plots of links (1) and (2) when we increased their initial angular velocities by 41% and 74%, respectively, as shown in Figure (5). The final initial values of the state variables used for the equivalent CBW model in MSC ADAMS are listed in Table (2) and compared with the initial values in MATLAB. Figure (6) shows the snapshots of a gait cycle of the final stable walking of the MSC ADAMS model.

5 Results and discussion

Here, the final results of the position, velocity, state errors, limit cycle phase diagram, Kinetic energy, Potential energy, and total mechanical energy are utilized to compare and validate the theoretical model in MATLAB and the physical model in MSC ADAMS. The outcomes of these comparisons are presented in Figures 7-10, respectively. Also, the geometric and physical quantities used in the theoretical model (MATLAB model) and physical model (MSC ADAMS model) are presented in Tables 1 and 2. As mentioned in the previous section, we have increased the initial angular velocities of the legs instead of the MATLAB model for the physical model of the CBW in MSC ADAMS to achieve stable periodic walking.
Figure (7) shows the plots of the angles and the angular velocities of the legs during periodic walking's five gait cycles (strides). As observed, the angles of the legs behave alternately to form consecutive steps in both plots. Note that the behavior of each of the angular velocities of the legs in a cycle differs between the stance and swing phases. It can be seen that the positions and velocities of the legs in both MSC ADAMS and MATLAB models are consistent with each other. We calculated the error between the theoretical model in MATLAB and the physical model in MSC ADAMS for both position and velocity data, as shown in Figure (8). As can be seen, the maximum error is around 10^{-4}, which indicates the effectiveness of MSC ADAMS modeling approach proposed here. In analyzing nonlinear systems, especially the dynamics of walking robots, the analysis of limit cycles is crucial. Figure (9) shows the phase diagram and limit cycles formed from simulation in MATLAB and MSC ADAMS. As seen, the limit cycles resulting from the outcomes of both the theoretical and physical models exhibit remarkably similar behavior, confirming the stability in the walking of both models.

To complete the comparison and validation between the theoretical model in MATLAB and the physical model in MSC ADAMS, the plots of the Kinetic, Potential, and total mechanical energies are also presented in Figure (10). They indicate that all energy components in both models align with each other well. As can be seen, both models have a significant difference between kinetic and potential energies. In fact, given the passive walking of the robot and the absence of controllers at the joints, it is reasonable for the numerical value of Kinetic energy to be very low.

Based on the results above, the critical characteristics of the two models have also been listed and quantitatively compared in Table (3). It is noteworthy that the average forward velocity of the robot's center of mass (v_{com}) is obtained by dividing the length of one complete step (Δx) by its time (t_{cycle}), where the length of the robot's step is constant and equal to 0.0342 meters for the periodic walking under study. As seen, the average velocity of the robot in both models is very close to each other, with a difference of less than 1%.

The two-link model assumed here is just a basic example to demonstrate the viability and general process of parameter adjustments for achieving dynamic consistency between ADAMS and MATLAB models. The same principles of validation and fine-tuning can be applied to more complex models, offering a general framework for dynamic modeling across different types of rigid-leg passive walkers in ADAMS.

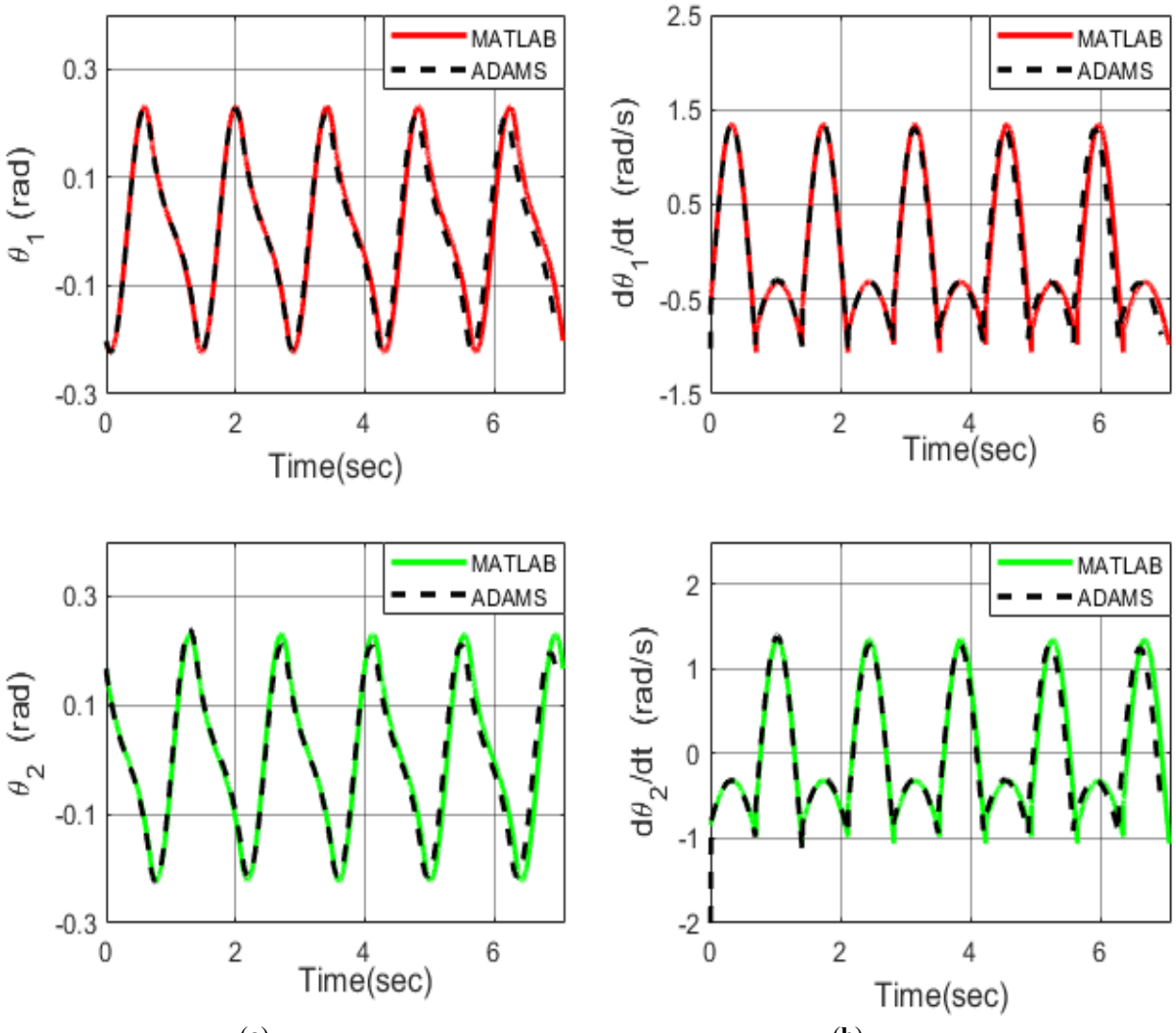

Figure 7 Comparing the results of CBW walking for five gait cycles or strides: **(a)** leg's angles, (**b**) leg's angular velocitie

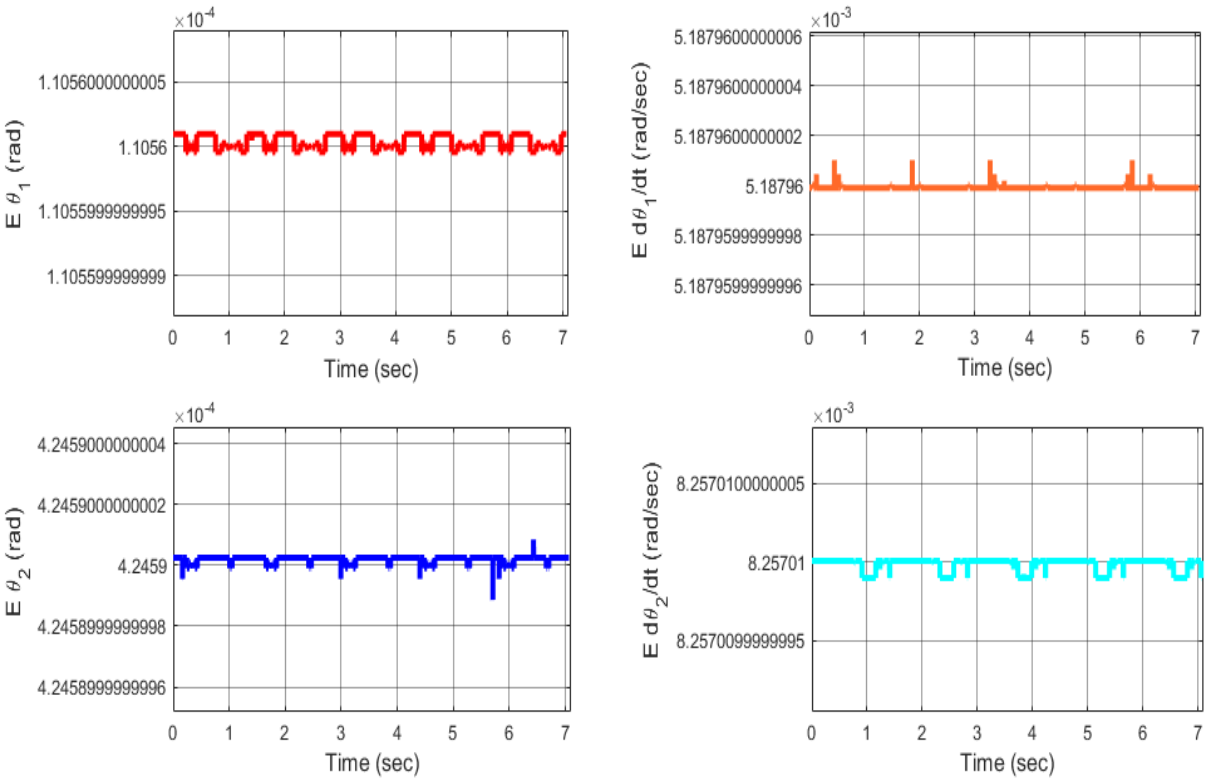

(**a**) (**b**)

Figure 8 Error between the results of MATLAB and MSC ADAMS model; (***a***) leg's angles and (**b**) leg's angular velocities

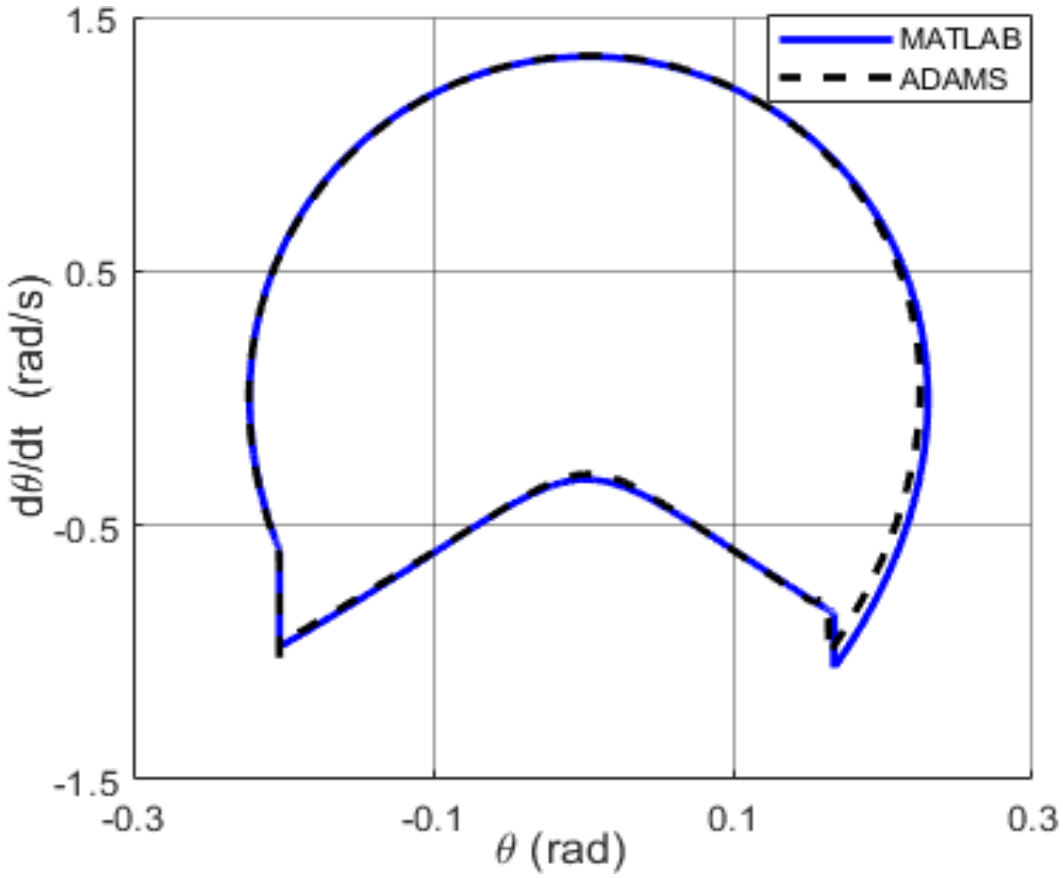

Figure 9 Limit cycles resulting from simulation in MATLAB and MSC ADAMS models

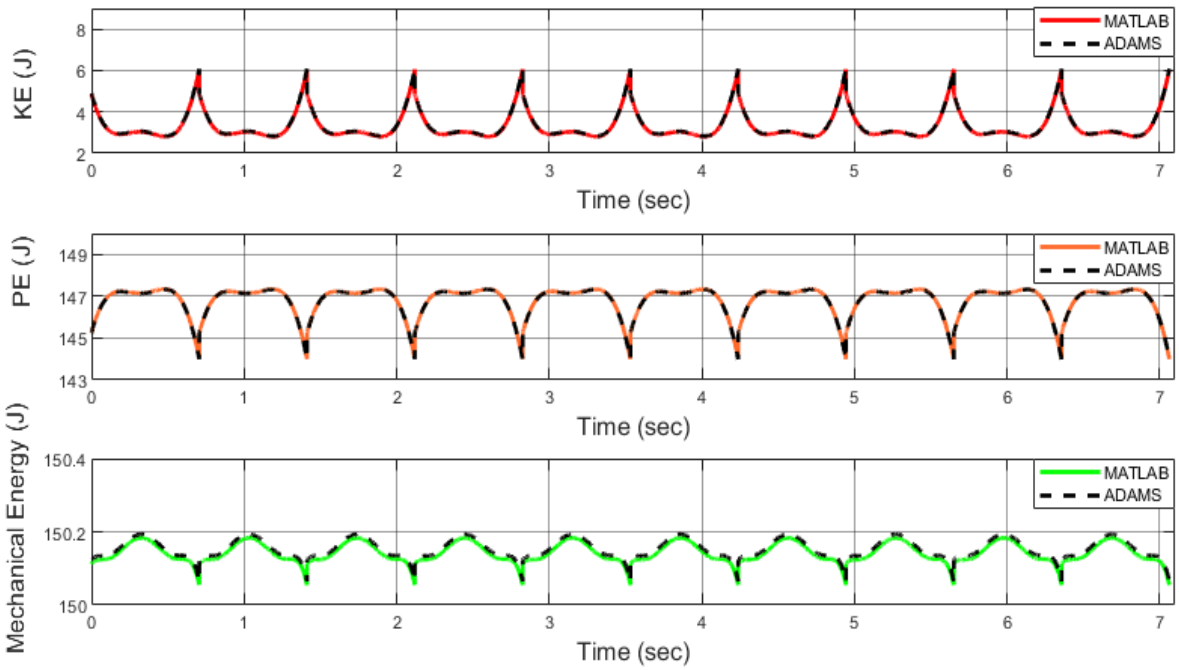

Figure 10 Kinematic, Potential, and Mechanical Energy compared between the model of MATLAB and MSC ADAMS

Table 3 Comparison of critical characteristics of MATLAB and ADAMS models for one step of periodic walking quantitively

Parameters	Symbol	Unit	MATLAB	MSC ADAMS
Left step period	t_{left}	(s)	0.60	0.59
Right step period	t_{right}	(s)	0.79	0.77
One cycle period	$t_{cycle} = t_{left} + t_{right}$	(s)	1.39	1.38
Average velocity of robot	$v_{com} = \Delta x / t_{cycle}$	(m/s)	0.0246	0.0248
Average mechanical energy (5 steps)	$E_{avg} = KE + PE$	(J)	150.13	150.14

6 Conclusion

This study presents a comprehensive modeling approach for passive biped walkers with rigid legs in MSC ADAMS. The research demonstrates the feasibility of physically modeling such passive walkers in MSC ADAMS while preserving fundamental properties such as speed, stride length, cycle, and natural dynamics similar to their full theoretical models. Guidelines for physical modeling in MSC ADAMS are developed and applied to achieve a match with the ideal theoretical model in MATLAB. In particular, as a parameter tuning, it was shown that a slightly higher initial angular velocity in MSC ADAMS is needed to compensate for the inevitable slippage of the stance foot at the beginning of motion, enabling periodic motion. The results highlight the effectiveness of the proposed approach in modeling an entirely theoretical compass biped in MSC ADAMS, similar to the ideal analytical model in MATLAB. By overcoming the challenges associated with the physical dynamic modeling of passive biped walkers, our approach not only simplifies and accelerates the construction of the passive biped models and their simulations but also provides a validation tool before conducting costly actual experiments.

This research lays the foundation for more accurate and reliable simulations of passive biped walkers, reducing reliance on purely theoretical models and providing a valuable tool for designing and developing these dynamic systems. The parameter adjustment of the ADAMS model described in this paper merely exemplifies the critical factors in achieving comparable results in ADAMS and MATLAB. It is evident that, by following the procedure presented in this paper, other researchers can easily establish their ADAMS model for any arbitrary passive walker in the future.

References

[1] C. Dinesh, M. Deivakani, P. Sunagar, R. Baskar, A. Kumar, and G. Kalra, "Biped Robot-based Walking on Uneven Terrain: Stability and Zero Moment Point (ZMP) Analysis," *in AIP Conference Proceedings*, 2023, Vol. 2831, No. 1: AIP Publishing, doi: https://doi.org/10.1063/5.0162762.

[2] J. W. Grizzle, G. Abba, and F. Plestan, "Asymptotically Stable Walking for Biped Robots: Analysis via Systems with Impulse Effects," *IEEE Transactions on Automatic Control*, Vol. 46, No. 1, pp. 51-64, 2001, doi: https://doi.org/10.1109/9.898695.

[3] E. R. Westervelt, J. W. Grizzle, and D. E. Koditschek, "Hybrid Zero Dynamics of Planar Biped Walkers," *IEEE Transactions on Automatic Control*, Vol. 48, No. 1, pp. 42-56, 2003, doi: https://doi.org/10.1109/TAC.2002.806653.

[4] J. W. Grizzle, and C. Chevallereau, "Virtual Constraints and Hybrid Zero Dynamics for Realizing Underactuated Bipedal Locomotion," *arXiv Preprint arXiv*:1706.01127, 2017, doi: https://doi.org/10.48550/arXiv.1706.01127.

[5] G. A. Castillo, B. Weng, W. Zhang, and A. Hereid, "Hybrid Zero Dynamics Inspired Feedback Control Policy Design for 3D Bipedal Locomotion using Reinforcement Learning," *in 2020 IEEE International Conference on Robotics and Automation (ICRA)*, IEEE, 2020, pp. 8746-8752, doi: https://doi.org/10.1109/ICRA40945.2020.9197175.

[6] M. S. Khan, and R. K. Mandava, "A Review on Gait Generation of the Biped Robot on Various Terrains," *Robotica*, Vol. 41, No. 6, pp. 1888-1930, 2023, doi: https://doi.org/10.1017/S0263574723000097.

[7] T. McGeer, "Passive Dynamic Walking," *The International Journal of Robotics Research*, Vol. 9, No. 2, pp. 62-82, 1990, doi: https://doi.org/10.1177/027836499000900206.

[8] T. McGeer, "Dynamics and Control of Bipedal Locomotion," *Journal of Theoretical Biology*, Vol. 163, No. 3, pp. 277-314, 1993, doi: https://doi.org/10.1006/jtbi.1993.1121.

[9] M. Garcia, A. Chatterjee, A. Ruina, and M. Coleman, "The Simplest Walking Model: Stability, Complexity, and Scaling," 1998, doi: https://doi.org/10.1115/1.2798313.

[10] A. Goswami, B. Thuilot, and B. Espiau, "Compass-like Biped Robot Part I: Stability and Bifurcation of Passive Gaits," *INRIA*, 1996, [Online], Available: https://inria.hal.science/inria-00073701

[11] X. Liu, H. Rong, F. Neri, vK. Zhang, Q. Yang, Z. Yu, and G. Zhang, "Human-simulated Intelligent Walking Control for Biped Robots," *IEEE Transactions on Automation Science and Engineering*, 2024, doi: https://doi.org/10.1109/TASE.2024.3391358.

[12] J. Giesbers, "Contact Mechanics in MSC ADAMS," 2012, [Online]. Available: https://purl.utwente.nl/essays/62109.

[13] J. Giesbers, "Contact Mechanics in MSC Adams-A Technical Evaluation of the Contact Models in Multibody Dynamics Software MSC Adams," 2012, [Online]. Available: https://purl.utwente.nl/essays/62109.

[14] N. Kalamain, and M. Farrokhi, "Dynamic Walking and Stepping over Large Obstacles of Biped Robots: A Poincaré Map Approach," *Journal of Engineering Science & Technology Review*, Vol. 15, No. 6, 2022, doi: http://dx.doi.org/10.25103/jestr.156.23.

[15] J. B. McConville, "Introduction to Mechanical System Simulation using Adams", SDC Publications, USA, 2015, ISBN-13: 978-1 -58503-988-3.

[16] S. H. Sadati, M. Borgheinejad, H. Fooladi, M. Naraghi, and A. Ohadi, "Optimum Design, Manufacturing and Experiment of a Passive Walking Biped: Effects of Structural Parameters on Efficiency, Stability and Robustness on Uneven Trains," *Applied Mechanics and Materials*, Vol. 307, pp. 107-111, 2013, doi: https://doi.org/10.4028/www.scientific.net/AMM.307.107.

[17] A. Çakan, and F. M. Botsalı, "Inverse Kinematics Analysis of a Puma Robot by using MSC Adams," *in Proceeding of The VIth International Conference Industrial Engineering and Environmental Protection*, Technical Faculty "Mihajlo Pupin" Zrenjanin, University of Novi Sad, Republic of Serbia, October, 3-4, 2016, pp. 274-277, doi: https://www.researchgate.net/publication/311953769_INVERSE_KINEMATICS_ANALYSIS_OF_A_PUMA_ROBOT_BY_USING_MSC_ADAMS.

[18] K. G. Aktas, F. Pehlivan, and I. Esen, "Kinematic Analysis of 4 Degrees of Freedom Robotic Arm and Simultaneous Trajectory Tracking using ADAMS®-MATLAB® Software," *in Proceeding of International Scientific and Vocational Studies Congress (BILMES 2017)*, 2017, doi: https://www.researchgate.net/publication/323855273_Kinematic_Analysis_of_4_Degrees_of_Freedom_Robotic_Arm_and_Simultaneous_Trajectory_Tracking_Using_ADAMSR-MATLABR_Software.

[19] C. Copilusi, S. Dumitru, I. Geonea, A. Margine, and D. Popescu, "Virtual Prototyping Validation of a Leg Exoskeleton Mechanism from Dynamic Considerations," *in International Conference Innovation in Engineering*, 2024, Springer, pp. 187-198, doi: https://doi.org/10.1007/978-3-031-62684-5_17.

[20] A. Abdulghani, M. Abdulsattar, and N. Abd al-sahib, "Study the Effect of Payload on Dynamic Simulation for Lower Limb Exoskeleton," *Chinese Journal of Computational Mechanics*, 2023, [Online]. Available: https://www.researchgate.net/publication/376073249_Study_the_Effect_of_Payload_on_Dynamic_Simulation_for_Lower_Limb_Exoskeleton.

[21] Y. Shi, M. Guo, R. Wang, D. Xia, X. Luo, X. Ji, and Y. Yang, "Modeling and Synergetic Simulation of a Lower Limb Exoskeleton Robot with the Human Subject," *in 2022 IEEE*

International Conference on Mechatronics and Automation (ICMA), IEEE, 2022, pp. 1493-1498, doi: https://doi.org/10.1109/ICMA54519.2022.9856355.

[22] M. Derman, A. F. Soliman, A. Kuru, S. C. Cevik, R. Unal, O. Bebek, and B. Ugurlu, "Simulation-based Design and Locomotion Control Implementation for a Lower Body Exoskeleton," i*n 2022 IEEE 5th International Conference on Industrial Cyber-physical Systems (ICPS)*, IEEE, 2022, pp. 1-6, doi: https://doi.org/10.1109/ICPS51978.2022.9816855.

[23] W. Li, K. Liu, C. Li, Z. Sun, S. Liu, and J. Gu, "Development and Evaluation of a Wearable Lower Limb Rehabilitation Robot," *Journal of Bionic Engineering*, Vol. 19, No. 3, pp. 688-699, 2022, doi: https://doi.org/10.1007/s42235-022-00172-6.

[24] A. S. Nair, and D. Ezhilarasi, "Performance Analysis of Super Twisting Sliding Mode Controller by ADAMS–MATLAB Co-simulation in Lower Extremity Exoskeleton," *International Journal of Precision Engineering and Manufacturing-green Technology*, Vol. 7, No. 3, pp. 743-754, 2020, doi: https://doi.org/10.1007/s40684-020-00202-w.

[25] M. C. Yildirim, P. Sendur, A. F. Soliman, and B. Ugurlu, "Optimal Stiffness Tuning for a Lower Body Exoskeleton with Spring-supported Passive Joints," *in 2018 7th IEEE International Conference on Biomedical Robotics and Biomechatronics (Biorob)*, IEEE, 2018, pp. 531-536, doi: https://doi.org/10.1109/BIOROB.2018.8487685.

[26] J. Suresh, K. S. Brahmanya, U. V. Kumar, and I. S. Beghel, "Analysis of Lower Body Exoskeleton using MSC ADAMS," [Online]. Available: https://www.ijeter.everscience.org/Manuscripts/Volume-5/Issue-12/Vol-5-issue-12-M-14.pdf.

[27] H. Wu, T. Jia, N. Li, J. Wu, and L. Yan, "Study on the Control Algorithm for Lower Limb Exoskeleton Based on ADAMS/Simulink Co-simulation," *Journal of Vibroengineering*, Vol. 19, No. 4, pp. 2976-2986, 2017, doi: https://doi.org/10.21595/jve.2017.17303.

[28] A. Margine, A. Ungureanu, P. Rinderu, and A. Dima, "Numerical Simulation and Experimental Characterization of a Leg Exoskeleton for Motion Assistance," *in Proceedings of the World Congress on Engineering*, 2017, Vol. 2, [Online]. Available: https://www.iaeng.org/publication/WCE2017/WCE2017_pp1013-1018.pdf.

[29] Z. C. Zhu, Z. Sui, Y. T. Tian, and H. Jiang, "Modeling and Control of Passive Dynamic Walking Robot with Humanoid Gait," *Applied Mechanics and Materials*, Vol. 461, pp. 903-907, 2014, doi: https://doi.org/10.4028/www.scientific.net/AMM.461.903.

[30] E. Hashemi, and A. Khajepour, "Kinematic and Three-dimensional Dynamic Modeling of A Biped Robot," *Proceedings of the Institution of Mechanical Engineers, Part K: Journal of Multi-body Dynamics*, Vol. 231, No. 1, pp. 57-73, 2017, doi: https://doi.org/10.1177/1464419316645243.

[31] L. Angel, C. Hernandez, and C. Diaz-Quintero, "Modeling, Simulation and Control of A Differential Steering Type Mobile Robot," i*n Proceedings of the 32nd Chinese Control Conference*, IEEE, 2013, pp. 8757-8762. [Online]. Available: https://ieeexplore.ieee.org/abstract/document/6640994.

[32] A. Mizani, V. E. Bejnordi, A. T. Safa, and M. Naraghi, "From Passive Dynamic Walking to Ankle Push-off Actuation: An MSC ADAMS Approach to Design," *in 2018 6th RSI International Conference on Robotics and Mechatronics (IcRoM)*, IEEE, 2018, pp. 400-405, doi: https://doi.org/10.1109/ICRoM.2018.8657640.

[33] M. R. da Silva, J. Coelho, F. Gonçalves, F. Novais, and P. Flores, "Multibody Dynamics in Robotics with Focus on Contact Events," *Robotica*, pp. 1-33, 2024, doi: https://doi.org/10.1017/S026357472400050X.

[34] J. J. Rond, M. C. Cardani, M. I. Campbell, and J. W. Hurst, "Mitigating Peak Impact Forces by Customizing the Passive Foot Dynamics of Legged Robots," J*ournal of Mechanisms and Robotics*, Vol. 12, No. 5, pp. 051010, 2020, doi: https://doi.org/10.1115/1.4046834.

[35] T. Ylikorpi, J.-L. Peralta, and A. Halme, "Comparing Passive Walker Simulators in MATLAB and ADAMS," *J. Struct. Mech*, Vol. 44, No. 1, pp. 65-92, 2011, doi: https://www.researchgate.net/publication/257696034_Comparing_passive_walker_simulators_in_MATLAB_and_ADAMS.

[36] C. Vasileiou, A. Smyrli, A. Drogosis, and E. Papadopoulos, "Development of a Passive Biped Robot Digital Twin using Analysis, Experiments, and a Multibody Simulation Environment," *Mechanism and Machine Theory*, Vol. 163, pp. 104346, 2021, doi: https://doi.org/10.1016/j.mechmachtheory.2021.104346.

[37] R. Ghanadi-Azar, M. R. Haghjoo, and M. Taghizadeh, "Parametric Study of Model-Based Dynamic Control Methods for Enhancing Locomotion in Underactuated Biped Robots. Case study: Hybrid Zero Dynamics and Proportional-Derivative Feedback," *Amirkabir Journal of Mechanical Engineering*, Vol. 56, No. 4, pp. 2-2, 2024, doi: https://doi.org/10.22060/mej.2024.22874.7688.

[38] W. Znegui, H. Gritli, and S. Belghith, "A New Poincaré Map for Investigating the Complex Walking Behavior of the Compass-Gait Biped Robot," *Applied Mathematical Modelling*, Vol. 94, pp. 534-557, 2021, doi: https://doi.org/10.1016/j.apm.2021.01.036.

[39] W. Znegui, H. Gritli, and S. Belghith, "Stabilization of the Passive Walking Dynamics of the Compass-gait Biped Robot by Developing the Analytical Expression of the Controlled Poincaré Map," *Nonlinear Dynamics*, Vol. 101, pp. 1061-1091, 2020, doi: https://doi.org/10.1007/s11071-020-05851-9.

[40] A. Smyrli, G. A. Bertos, and E. Papadopoulos, "Efficient Stabilization of Zero-slope Walking for Bipedal Robots Following their Passive Fixed-point Trajectories," *in 2018 IEEE International Conference on Robotics and Automation (ICRA)*, IEEE, 2018, pp. 5733-5738, doi: https://doi.org/10.1109/ICRA.2018.8460845.

[41] W. Y. Yang, W. Cao, J. Kim, K. W. Park, H. H. Park, J. Joung, J. S. Ro, H. L. Lee, C. H. Hong, and T. Im, "Applied Numerical Methods using MATLAB," 2020, doi: 10.1002/9781119626879.

[42] R. V. Dukkipati, "*Applied Numerical Methods using MATLAB*," Mercury Learning & Information, 2023, ISBN: 978-1-68392-868-3.

[43] C. Lopez, "MATLAB Optimization Techniques," 2014, doi: https://doi.org/10.1007/978-1-4842-0292-0.

[44] Z. Wei, J. Chen, G. Jin, D. Liang, and Z. Wang, "Research on Dynamic Analysis and Simulation of Cam Mechanism Considering Contact Collision," *Iranian Journal of Science and Technology, Transactions of Mechanical Engineering*, pp. 1-14, 2023, doi: https://doi.org/10.1007/s40997-023-00703-4.

[45] K.-H. Chang, Motion Simulation and Mechanism Design with SOLIDWORKS Motion 2023. *SDC publications*, 2023.

[46] J. Giesbers, "J. Giesbers, "Contact Mechanics in MSC Adams: A Technical Evaluation of the Contact Models in Multibody Dynamics Software MSC Adams," B.S. Thesis, Faculty of Engineering Technology, Applied Mechanics, University of Twente, Enschede, The Netherlands, 2012, [Online]. Available: https://purl.utwente.nl/essays/62109.

[47] D. Sosa-Méndez, E. Lugo-González, M. Arias-Montiel, and R. A. Garcia-Garcia, "ADAMS-MATLAB Co-simulation for Kinematics, Dynamics, and Control of the Stewart–Gough Platform," *International Journal of Advanced Robotic Systems*, Vol. 14, No. 4, pp. 1729881417719824, 2017, doi: https://doi.org/10.1177/1729881417719824.

Appendix A

This section illustrates the equations of motion for a compass biped robot. The introduction of the physical and geometrical model is in section 2. In the following equations, $\boldsymbol{p_{\theta_2}}, \boldsymbol{p_{\theta_1}}, \boldsymbol{p_{MH}}$ are the position of the centers of mass of the legs and the hip, and additionally, $\boldsymbol{v_{\theta_2}}, \boldsymbol{v_{\theta_1}}, \boldsymbol{v_{MH}}$ are angular velocities.

$$\boldsymbol{p_{\theta_2}} = \begin{bmatrix} -a \times sin(\theta_2) \\ a \times cos(\theta_2) \end{bmatrix} \tag{A.1}$$

$$\boldsymbol{p_{MH}} = \begin{bmatrix} -L \times sin(\theta_2) \\ L \times cos(\theta_2) \end{bmatrix} \tag{A.2}$$

$$\boldsymbol{p_{\theta_1}} = \boldsymbol{p_{MH}} + \begin{bmatrix} b \times sin(\theta_1) \\ -b \times cos(\theta_1) \end{bmatrix} \tag{A.3}$$

$$\boldsymbol{D} = \begin{bmatrix} m \times b^2 & -m \times L \times b \times cos(\theta_2 - \theta_1) \\ -m \times L \times b \times cos(\theta_2 - \theta_1) & MH \times L^2 + m \times (L^2 + a^2) \end{bmatrix} \tag{A.4}$$

$$\boldsymbol{C} = \begin{bmatrix} 0 & m \times L \times b \times \dot{\theta_2} \times sin(\theta_2 - \theta_1) \\ m \times L \times b \times \dot{\theta_1} \times sin(\theta_2 - \theta_1) & 0 \end{bmatrix} \tag{A.5}$$

$$\boldsymbol{G} = \begin{bmatrix} m \times g \times b \times \sin(\theta_1) \\ -(MH \times L + m * (a + L)) \times g \times \sin(\theta_2) \end{bmatrix} \tag{A.6}$$

$$\boldsymbol{D_e} = \begin{bmatrix} D_{e_{11}} & D_{e_{12}} & D_{e_{13}} & D_{e_{14}} \\ D_{e_{21}} & D_{e_{22}} & D_{e_{23}} & D_{e_{24}} \\ D_{e_{31}} & D_{e_{32}} & D_{e_{33}} & D_{e_{34}} \\ D_{e_{41}} & D_{e_{42}} & D_{e_{43}} & D_{e_{44}} \end{bmatrix}, \boldsymbol{C_e} = \begin{bmatrix} C_{e_{11}} & C_{e_{12}} & C_{e_{13}} & C_{e_{14}} \\ C_{e_{21}} & C_{e_{22}} & C_{e_{23}} & C_{e_{24}} \\ C_{e_{31}} & C_{e_{32}} & C_{e_{33}} & C_{e_{34}} \\ C_{e_{41}} & C_{e_{42}} & C_{e_{43}} & C_{e_{44}} \end{bmatrix}, \tag{A.7}$$

$$\boldsymbol{G_e} = \begin{bmatrix} b \times g \times m \times sin(\theta_1) \\ -g \times sin(\theta_2) \times (L \times m + a \times m + L \times MH) \\ 0 \\ g \times (MH + 2 \times m) \end{bmatrix} \tag{A.8}$$

$$D_{e_{11}} = m \times b^2 \tag{A.9}$$

$$D_{e_{12}} = -m \times L \times b \times cos(\theta_2 - \theta_1) \tag{A.10}$$

$$D_{e_{13}} = b \times m \times \cos(\theta_1) \tag{A.11}$$

$$D_{e_{14}} = b \times m \times \sin(\theta_1) \tag{A.12}$$

$$D_{e_{21}} = -m \times L \times b \times cos(\theta_2 - \theta_1) \tag{A.13}$$

$$D_{e_{22}} = L^2 \times MH + L^2 \times m + a^2 \times m \tag{A.14}$$

$$D_{e_{23}} = -\cos(\theta_2) \times (L \times m + a \times m + L \times MH) \tag{A.15}$$

$$D_{e_{24}} = -\sin(\theta_2) \times (L \times m + a \times m + L \times MH) \tag{A.16}$$

$$D_{e_{31}} = b \times m \times \cos(\theta_1) \tag{A.17}$$

$$D_{e_{32}} = -\cos(\theta_2) \times (L \times m + a \times m + L \times MH) \tag{A.18}$$

$$D_{e_{33}} = MH + 2 \times m \tag{A.19}$$

$$D_{e_{34}} = 0 \tag{A.20}$$

$$D_{e_{41}} = b \times m \times sin(\theta_1) \tag{A.21}$$

$$D_{e_{42}} = -\sin(\theta_2) \times (L \times m + a \times m + L \times MH) \tag{A.22}$$

$$D_{e_{43}} = 0 \tag{A.23}$$

$$D_{e_{44}} = MH + 2 \times m \tag{A.24}$$

$$C_{e_{11}} = 0 \tag{A.25}$$

$$C_{e_{12}} = -m \times L \times b \times \dot{\theta}_2 \times sin(\theta_1 - \theta_2) \tag{A.26}$$

$$C_{e_{13}} = 0 \tag{A.27}$$

$$C_{e_{14}} = 0 \tag{A.28}$$

$$C_{e_{21}} = -m \times L \times b \times \dot{\theta}_1 \times sin(\theta_1 - \theta_2) \tag{A.29}$$

$$C_{e_{22}} = 0 \tag{A.30}$$

$$C_{e_{23}} = 0 \tag{A.31}$$

$$C_{e_{24}} = 0 \tag{A.32}$$

$$C_{e_{31}} = -b \times \dot{\theta}_1 \times m \times \sin(\theta_1) \tag{A.33}$$

$$C_{e_{32}} = \dot{\theta}_2 \times \sin(\theta_2) \times (L \times m + a \times m + L \times MH) \tag{A.34}$$

$$C_{e_{33}} = 0 \tag{A.35}$$

$$C_{e_{34}} = 0 \tag{A.36}$$

$$C_{e_{41}} = b \times \dot{\theta}_1 \times m \times \cos(\theta_1) \tag{A.37}$$

$$C_{e_{42}} = -\dot{\theta}_2 \times \cos(\theta_2) \times (L \times m + a \times m + L \times MH \tag{A.38}$$

$$C_{e_{43}} = 0 \tag{A.39}$$

$$C_{e_{44}} = 0 \tag{A.40}$$

$$\boldsymbol{D_e \dot{q}_e}^{+} - \boldsymbol{D_e \dot{q}_e}^{-} = \boldsymbol{F_{ext}} \tag{A.41}$$

In the above equation, $\boldsymbol{\dot{q}_e}^{-}$ represents the velocities before impact, and $\boldsymbol{\dot{q}_e}^{+}$ represents the velocities after the leg's impact on the ground.

$$\boldsymbol{P(q_e)} = \begin{bmatrix} x + L(sin(\theta_1) + sin(-\theta_2)) \\ y + L(cos(\theta_1) - cos(-\theta_2)) \end{bmatrix} \tag{A.55}$$

$$\boldsymbol{E} = \frac{\boldsymbol{\partial}}{\boldsymbol{\partial q_e}} \boldsymbol{P(q_e)} \tag{A.56}$$

$$\begin{bmatrix} \boldsymbol{D_e}_{4\times4} & \boldsymbol{(-E)'}_{4\times2} \\ \boldsymbol{E}_{2\times4} & \boldsymbol{0}_{2\times2} \end{bmatrix} \begin{bmatrix} \boldsymbol{\dot{q}_e}^{+}{}_{4\times1} \\ \boldsymbol{F}_{2\times1} \end{bmatrix} = \begin{bmatrix} \boldsymbol{(D_e \times \dot{q}_e}^{-})_{4\times1} \\ \boldsymbol{0}_{2\times1} \end{bmatrix} \tag{A.57}$$

$$\boldsymbol{f(x)} = \begin{bmatrix} \dot{\boldsymbol{q}} \\ \boldsymbol{D^{-1}(-C\dot{q} - G)} \end{bmatrix} \tag{A.58}$$